SCIENCE CHINA
Physics, Mechanics & Astronomy

• Article •

December 2016 Vol. 59 No. 12: 122011
doi: 10.1007/s11433-016-0358-y

Influence of the time-step on the production of free nucleons and pions from heavy-ion collisions around 1 GeV/nucleon

LiYan Zou[1,2], Miao Li[1,2], ChenChen Guo[3], YongJia Wang[1*], QingFeng Li[1,4*], and Ling Liu[2]

[1] *School of Science, Huzhou University, Huzhou 313000, China;*
[2] *College of Physics Science and Technology, Shenyang Normal University, Shenyang 110034, China;*
[3] *Shanghai Institute of Applied Physics, Chinese Academy of Sciences, Shanghai 201800, China;*
[4] *Institute of Modern Physics, Chinese Academy of Sciences, Lanzhou 730000, China*

Received September 5, 2016; accepted October 8, 2016; published online October 25, 2016

By considering different values of the time-step for the potential updates in the ultra-relativistic quantum molecular dynamics (UrQMD) model, we examine its influence on observables, such as the yield and collective flow of nucleons and pions from heavy-ion collisions around 1 GeV/nucleon. It is found that these observables are affected to some extent by the choice of the time-step, and the impact of the time-step on the pion-related observables is more visible than that on the nucleon-related ones. However, its effect on the π^-/π^+ yield ratio and elliptic flow difference between neutrons and protons, which have been taken as sensitive observables for probing the density-dependent nuclear symmetry energy at high densities, is fairly weak.

UrQMD model, symmetry energy at supranormal densities, mean-field potential updates

PACS number(s): 21.65.Cd, 21.65.Mn, 25.70.-z

Citation: L. Y. Zou, M. Li, C. C. Guo, Y. J. Wang, Q. F. Li, and L. Liu, Influence of the time-step on the production of free nucleons and pions from heavy-ion collisions around 1 GeV/nucleon, Sci. China-Phys. Mech. Astron. **59**, 122011 (2016), doi: 10.1007/s11433-016-0358-y

1 Introduction

The nuclear symmetry energy is an important quantity not only because it relates to the properties of nuclei with large isospin asymmetry but also because it influences to a great extent the mass-radius relation of neutron stars in the universe [1-3]. For the past few decades many attempts have been made to extract information of the nuclear symmetry energy from both nuclei-related quantities and neutron star observations. However, a complete picture of the density dependence of the nuclear symmetry energy $E_{\rm sym}(\rho)$ still has not been obtained so far [4-14]. The most probable way on the earth to probe the $E_{\rm sym}(\rho)$ at high densities is by heavy-ion collisions (HICs). Nevertheless, it can not be measured directly but only extracted indirectly from a comparison between experimental measured data and the corresponding transport model simulations. Therefore, the transport model plays a crucial role. However, the $E_{\rm sym}(\rho)$ extracted from the same data but with different transport models are sometimes inconsistent with each other, or even contradictory [15-20]. For example, comparing the same π^-/π^+ yield ratio data measured by FOPI Collaboration, both the isospin-dependent Boltzmann-Uehling-Uhlenbeck (IBUU) model and the improved isospin-dependent Boltzmann-Langevin model favor a soft symmetry energy ($E_{\rm sym}$ increases slowly as density increasing and/or even decrease at high densities), while the Lanzhou quantum molecular dynamics (LQMD) model supports a very stiff symmetry energy ($E_{\rm sym}$ increases rapidly as density increasing). It is important to note that reliable results can be extracted from a comparison between the experimental data and the transport model simulations only if

*Corresponding authors (YongJia Wang, email: wangyongjia@zjhu.edu.cn;
QingFeng Li, email: liqf@zjhu.edu.cn)

the calculation is not (largely) affected by some model uncertainties/parameters. Unfortunately, in the recent transport code comparison project, even when the same physics inputs (such as mean filed potentials and nucleon-nucleon cross sections) are chosen, results from the 18 commonly used codes are still distinct [21]. Thus a detailed examination of the effect of various assumptions/parameters/uncertainties used in transport models on observables is still on the way.

In our recent progress, the effect of the spin-orbit interaction [22] and inner magnetic field [23] on collective flows in heavy-ion collisions at intermediate energies are surveyed. In this work one more uncertainty coming from the time-step related parameter used for potential updates in the mean-field part is further examined. And, in this procedure, the positions $\boldsymbol{r}$ and momenta $\boldsymbol{p}$ of particles are updated via Hamilton's equations, $\mathrm{d}\boldsymbol{r}/\mathrm{d}t = \nabla_{\boldsymbol{p}} H$ and $\mathrm{d}\boldsymbol{p}/\mathrm{d}t = -\nabla_{\boldsymbol{r}} H$. The Euler method is usually employed to solve these differential equations with given initial values of the phase space, $\boldsymbol{r}_{(t+\Delta t)} = \boldsymbol{r}_{(t)} + \nabla_{\boldsymbol{p}} H \Delta t$ and $\boldsymbol{p}_{(t+\Delta t)} = \boldsymbol{p}_{(t)} - \nabla_{\boldsymbol{r}} H \Delta t$, here Δt is the time-step required in transport codes [24, 25]. Sometimes, a high-order numerical method is adopted in calculations for a higher precision but the choice of the Δt value is inevitable. In principle, a smaller value of Δt gives a more accurate result, but increases much more computational time. Therefore, Δt= 0.5 and 1.0 fm/c are usually adopted (although relatively arbitrarily) for observables from HICs at beam energies ranging from several tens of MeV/nucleon up to several GeV/nucleon. Thus two questions are being arised concerning the selection of the time-step: (1) How does the time-step influence observables in HICs? (2) In particular, whether does it have any influence upon some isospin-sensitive observables?

In this work, with the ultrarelativistic quantum molecular dynamics (UrQMD) model, we investigate the influence of the time-step on the yield and the collective flow of nucleons and pions, as well as the related isospin-sensitive observables, e.g., the elliptic flow difference between protons and neutrons and the π^-/π^+ yield ratio. In the next section, the transport model and collective flow used in this work are briefly introduced. Then, calculations and analyses are shown in sect. 3. Finally, a summary is given in sect. 4.

2 Description of the UrQMD model and the collective flow

The UrQMD model [26, 27] is based on the same principles as the quantum molecular dynamics (QMD) in which nucleons are represented by a Gaussian wave packets in configuration and momentum space [28]. It inherits the mean field part from the QMD model and the two-body collision part from the relativistic quantum molecular dynamics (RQMD) model [29]. It can be employed in studying nuclear reactions of p+p, p+A and A+A systems within a large range of beam energies, from several tens of MeV/nucleon up to the highest energy available at the CERN large hadron collider (LHC). In recent years, following up the recent progress in determining the nuclear symmetry energy, the Skyrme potential energy density functional has been incorporated into the UrQMD code in order to consider a very soft nuclear symmetry energy which can not be expressed by a simple power-law dependence on density (i.e., $E_{\mathrm{sym}}(\rho) = 12(\rho/\rho_0)^{2/3} + C_p(\rho/\rho_0)^{\gamma}$). With the further help of the medium-modified nucleon-nucleon elastic cross sections in the collision part and an isospin-dependent minimum span tree (iso-MST) algorithm in the coalescence process, the recently published experimental data from the INDRA and FOPI collaborations at GSI can be reproduced rather well [30-33]. In this work, the SV-mas08 and SkI1 Skyrme interactions [34] are chosen in which the incompressibility K_0 = 233 and 243 MeV, and the slope parameter of nuclear symmetry energy L = 40 (soft) and 161 MeV (stiff), respectively.

The collective flow is one of most important and commonly used observables in HICs over a wide beam energy range, which reflects the collective motions of emitted particles and then provides a chance to investigate some important quantities, such as the stiffness of the nuclear equation of state (EoS) and the medium modifications of the nucleon-nucleon cross section. The directed and elliptic flow parameters v_1 and v_2 are the first- and second- order coefficients of a Fourier expansion of the azimuthal particle distribution and can be further expressed as follows (see ref. [35] for details):

$$v_1 \equiv \langle \cos(\phi) \rangle = \left\langle \frac{p_x}{p_t} \right\rangle; v_2 \equiv \langle \cos(2\phi) \rangle = \left\langle \frac{p_x^2 - p_y^2}{p_t^2} \right\rangle, \quad (1)$$

here p_x and p_y are the two components of the transverse momentum $p_t = \sqrt{p_x^2 + p_y^2}$. The angular brackets denote an average over all considered particles from all events. In general, both the directed flow v_1 and elliptic flow v_2 are functions of the p_t and the normalized longitudinal rapidity rapidity y_0 ($\equiv y_z/y_{\mathrm{pro}}$, where $y_z = \frac{1}{2} \ln \frac{E+p_z}{E-p_z}$ and the subscript pro denotes the incident projectile in the center-of-mass system) from a colliding system with certain beam energy E_{lab} and impact parameter b [or, the reduced one defined as $b_0 = b/b_{\mathrm{max}}$ with $b_{\mathrm{max}} = 1.15(A_P^{1/3} + A_T^{1/3})$.

In addition, in order to construct clusters as well as free nucleons at the final stage (the stopping time for UrQMD calculations is set to 100-150 fm/c depending on the selection of the beam energy), the iso-MST coalescence model [33,36] is employed, in which two essential parameters related to the relative distance $\delta r < R_0$ (which is isospin dependent and $R_0^{\mathrm{nn}} = R_0^{\mathrm{np}} = 3.8$ fm and $R_0^{\mathrm{pp}} = 2.8$ fm) and the relative momentum $\delta p < P_0$ (where $P_0 = 0.25$ GeV/nucleon) are chosen loosely because in this work a precise comparison between calculations and experimental data is not pursued.

3 Results and discussions

3.1 Yields of free nucleons and pions

The production of free nucleons and pions in HICs at inter-

mediate energies has attracted much attention in recent decades partly due to its potential application to constrain the poorly known density-dependent nuclear symmetry energy. In Figure 1, yields of free nucleons and total pions produced from central (b_0 < 0.15) Au+Au collisions at the beam energies 0.4 (squares), 1.0 (circles) and 1.5 (triangles) GeV/nucleon are shown as a function of the time-step. The SV-mas08 Skyrme interaction is used for calculations (the same below except otherwise stated). In order to assess the influence of time-step on HICs, Δt=0.25 fm/c is added for Au+Au collisions at 1.0 and 1.5 GeV/nucleon, besides 0.5, 1.0, and 2.0 fm/c. It can be seen that the yield of free nucleons is hardly affected by the time-step (guided by the linearly fitting lines), whereas the pion yields visibly decrease as the Δt shortens (e.g., at 0.4 GeV/nucleon, the total yield of pions using Δt=0.5 fm/c is about 20% smaller than that when Δt=2.0 fm/c).

It is known that the pion production is directly correlated to the decay of Δ resonances, which are mainly created from the nucleon-nucleon inelastic NN → NΔ process at beam energies used in this work. Thus it is necessary to check the influence of the time-step on different reaction channels. As shown in Figure 2, the numbers of NN elastic (a) and inelastic scattering channels as well as the Δ absorption channel (b) in central (b = 1 fm) Au+Au collisions at the beam energy 1.0 GeV/nucleon are collected within different time-steps. In addition, the collision number difference between the NN inelastic and the Δ absorption channels is also shown in the rightmost place in order to observe the "net" production of

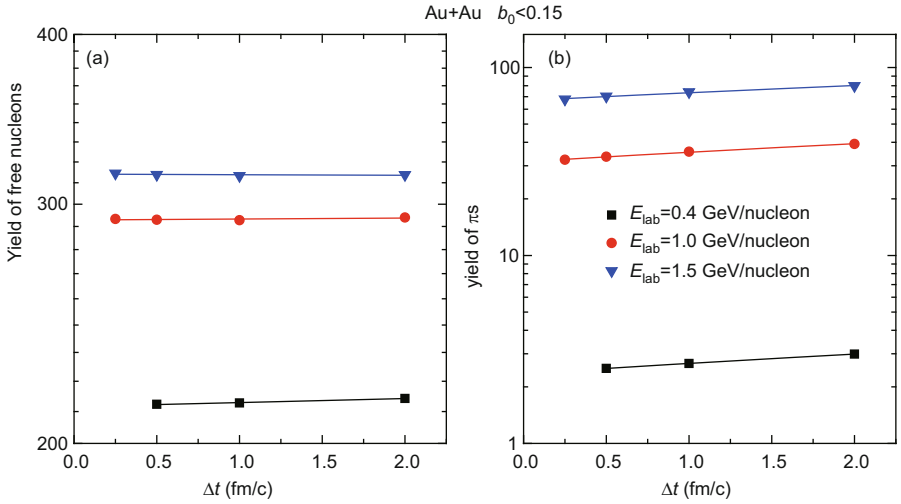

Figure 1 (Color online) The yields of free nucleons (a) and pions (b) from central (b_0 < 0.15) Au+Au collisions at the beam energies 0.4 (squares), 1.0 (circles), and 1.5 GeV/nucleon (triangles) as a function of the time-step Δt. The solid lines in both plots are linear fits to the UrQMD calculations.

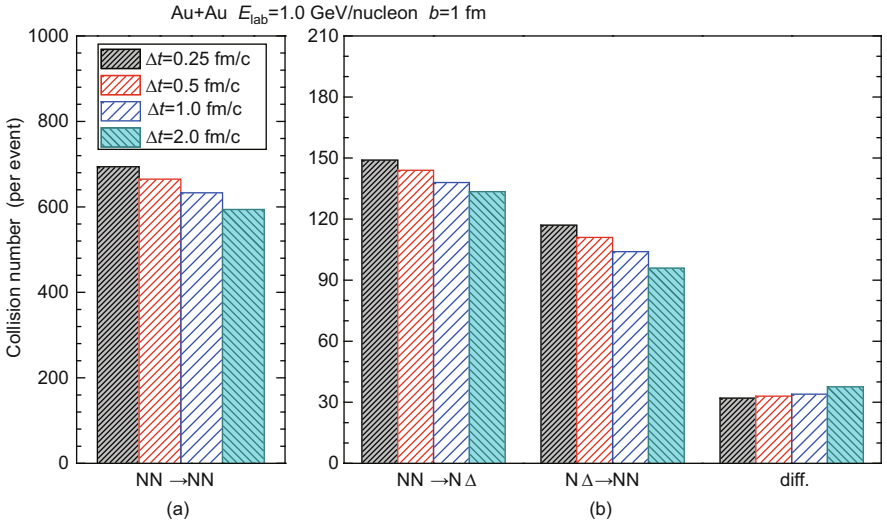

Figure 2 (Color online) The collision numbers of elastic NN → NN (a), inelastic NN → NΔ and NΔ → NN processes (b), as well as the difference (diff.) between the NN → NΔ and NΔ → NN channels (rightmost) in central (b = 1 fm) Au+Au collisions at E_{lab} = 1.0 GeV/nucleon, as calculated with different time-steps shown by different bars.

Δs if other inelastic channels are neglected. First, we can see that the collision numbers for these three channels decrease monotonously as Δt increases, which is understandable since a larger Δt leads to an earlier emission of particles from the compressed center, so that the probability of collisions is driven down accordingly. However, the number difference between the NN $\rightarrow$ NΔ and NΔ $\rightarrow$ NN collisions is seen to increase with increasing Δt, so as to the increase of pion yield as shown in Figure 1.

3.2 Collective flows of protons and pions

Besides the multiplicity, the collective flow of particles is another essential observable in HICs over a wide range of beam energies. It is found that the choice of time-step in $\Delta t < 2$ fm/c does not visibly change values of the directed (v_1) and elliptic (v_2) flows of free protons and pions from Au+Au collisions at the low beam energy such as 0.4 GeV/nucleon, while it does when $E_{\rm lab}$ increases to, e.g., 1 GeV/nucleon. Figures 3 and 4 respectively display the v_1 and v_2 of free protons and charged pions produced from semi-peripheral (b= 7 fm) Au+Au collisions at 1.0 GeV/nucleon. Calculations with Δt = 0.25, 0.5, and 1 fm/c are shown with lines (the same below except otherwise stated). From Figure 3, one can see clearly that the v_1 of protons (Figuer 3(a)) is still not changed with varying Δt but its absolute value of v_2 at mid-rapidity (Figure 3(b)) is apparently increased when the value of Δt increases from 0.25 to 1.0 fm/c ($\sim$ 10%). As for flows of pions shown in Figure 4, it is seen firstly that the slope of v_1 of π^- (π^+) at mid-rapidity is positive (negative), and meanwhile the v_2 of π^+ is smaller than that of π^-, which are mainly due to the effect of the Coulomb potential between pions and protons [37] and are consistent with the FOPI experimental data with nearby conditions [38] as well. Further, the time-step effect on flows of pions is similar to but relatively larger than that on flows of nucleons. For example, the enhancement of the absolute value of v_2 for π^+ at mid-rapidity from Δt=0.25 to 1.0 fm/c is about 16%, while that for protons is about 11%. The trend of a smaller absolute value of v_2 of both nucleons and pions with a smaller Δt can be understood from the fact that the increased collision number for a smaller Δt seen from Figure 2 leads to a more isotropic emission.

Furthermore, in Figures 3 and 4 the large influence of the time-step on the elliptic flow especially at mid-rapidity is due to the strong effect of mean-field potentials in the central high-density region and can be more clarified from its transverse-momentum dependence. Figure 5 depicts the elliptic flow of free protons (a), π^- s (b), and π^+ s (in (c)) as a function of the transverse momentum p_t. A middle rapidity cut $-0.4 < y_0 < 0.4$ is chosen. It is seen clearly that the impact of the time-step on the elliptic flow becomes more visible at higher p_t. We also find from Figures 3-5 that both the rapidity- and the transverse-momentum dependence of v_1 and v_2 flows for both nucleons and pions with a time-step Δt = 0.5 fm/c are very close to those with Δt = 0.25 fm/c. In order to save the valuable computational time, Δt=0.5 fm/c is short enough for simulating HICs at beam energies around 1.0 GeV/nucleon.

3.3 Elliptic flow difference between neutrons and protons $v_2^{\rm n}$-$v_2^{\rm p}$ and charged pion yield ratio π^-/π^+

However, it is still curious to see how the effect of the time-step on sensitive observables related to the density dependence of symmetry energy since the symmetry energy is a secondary correction to the EoS of the nuclear matter under normal conditions. Figures 6 and 7 show respectively the elliptic flow difference v_2^n-v_2^p of free neutrons and protons and the charged pion yield ratio π^-/π^+ as a function of the rapidity. Two Skyrme potentials and two Δt values are chosen and distinguished by different lines. It is seen clearly that, in the

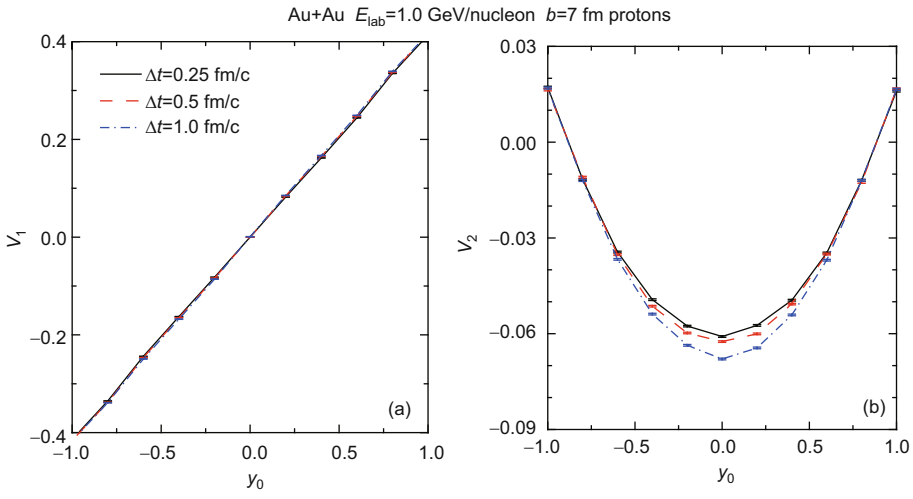

Figure 3 (Color online) The rapidity distributions of the directed (a) and elliptic (b) flows of free protons produced from semi-peripheral (b=7 fm) Au+Au collisions at 1.0 GeV/nucleon. Calculations performed with different time-steps are distinguished by different lines.

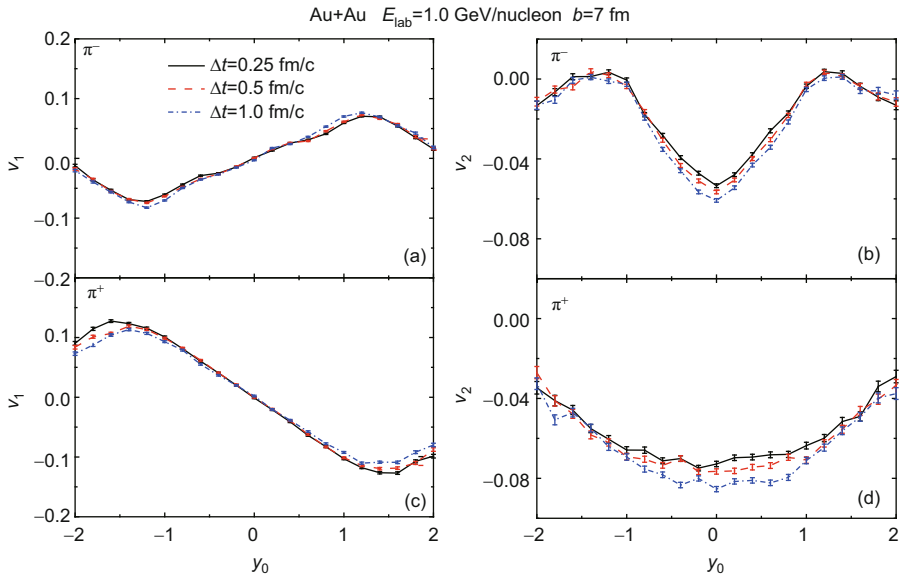

Figure 4 (Color online) The same as Figure 3 but for π^- (upper plots) and π^+ mesons (lower plots).

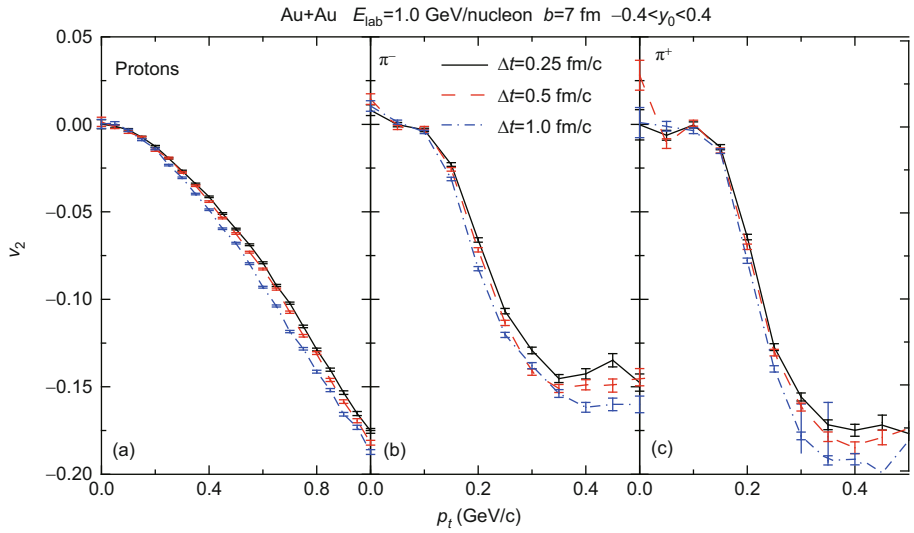

Figure 5 (Color online) The transverse momentum distributions of the elliptic flow of free protons (in plot (a)), π^- s (in (b)), and π^+ s (in (c)) from semi-peripheral (b=7 fm) Au+Au collisions at 1.0 GeV/nucleon. The rapidity cut $-0.4 < y_0 < 0.4$ is chosen.

concerned rapidity region $-1.0 < y_0 < 1.0$, these calculation results are sensitive to the choice of the stiffness of the symmetry energy represented respectively by the SV-mas08 with a small L value and the SkI1 with a large L value, as stated before. But, the time-step effect is eliminated almost entirely, which is due to the fact that the change of both yields and flows of separate particles with increasing Δt is with the same trend and quantitatively quite similar to each other. We have also found that, at a lower beam energy such as 0.4 GeV/nucleon where these observables show a larger isospin effect, this conclusion is still perfectly guaranteed. Hence, the large cancellation related to Δt shown in Figures 6 and 7 confirms that another source of the systematic uncertainties when extracting the density dependence of the symmetry energy at high densities can be removed with safety.

4 Summary

In summary, within the ultrarelativistic quantum molecular dynamics (UrQMD) model, the influence of the time-step Δt for the update of the mean field potentials on the production and collective flow of nucleons and pions from ^{197}Au+^{197}Au collisions at E_{lab}=0.4, 1.0, and 1.5 GeV/nucleon is studied. As Δt increases from 0.25 to 2 fm/c, it is found that the yield of free nucleons can hardly be affected by the time-step, while the pion yield is visibly enhanced especially at low beam energies. This enhancement is as a consequence of the rise in the collision number difference between the NN→NΔ and the

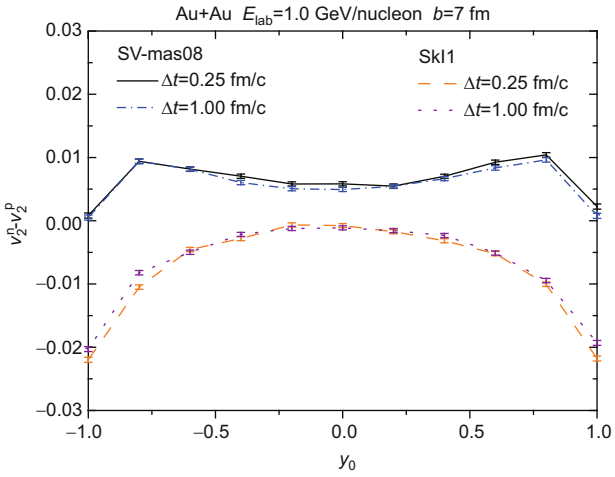

Figure 6 (Color online) Rapidity dependence of the elliptic flow difference (v_2^n-v_2^p) between free neutrons and protons. Calculations are obtained with two Skyrme potentials (SV-mas08 and SkI1) and two values of the time-step for semi-peripheral (b=7 fm) Au+Au collisions at 1.0 GeV/nucleon.

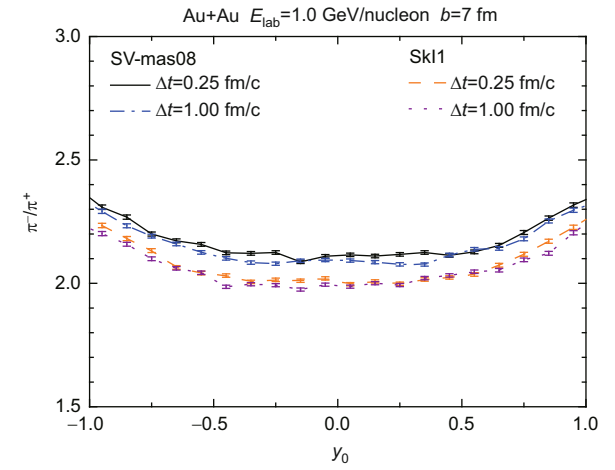

Figure 7 (Color online) The same as Figure 6 but for the yield ratio of π^- and π^+ mesons.

inverse N$\Delta \rightarrow$ NN processes, although both of them are decreased monotonously with increasing Δt. The visible influence of the Δt on the collective flow is also seen especially on the v_2 values of nucleons and pions at a high energy such as 1 GeV/nucleon. In order for a good accuracy, and taking into account a fast computational speed, a relatively small value of Δt=0.5 fm/c is suitable for simulating HICs at beam energies around 1 GeV/nucleon. And, because of the large cancellation effect, both the elliptic flow difference v_2^n-v_2^p between neutrons and protons and the π^-/π^+ yield ratio, which are suggested as sensitive observables for probing the density-dependent symmetry energy at high densities, are invisibly affected by the choice of Δt value.

This work was supported by the National Natural Science Foundation of China (Grant Nos. 11505057, 11547312, 11375062, and 11605270), the Department of Education of Zhejiang Province (Grant No. Y201533176), and the China Postdoctoral Special Science Foundation (Grant No. 2016M591730). The authors acknowledge support by the computing server C3S2 in Huzhou University.

1 A. W. Steiner, M. Prakash, J. M. Lattimer, and P. J. Ellis, Phys. Rept. **411**, 325 (2005).
2 J. M. Lattimer, and M. Prakash, Phys. Rept. **442**, 109 (2007).
3 B. A. Li, L. W. Chen, and C. M. Ko, Phys. Rep. **464**, 113 (2008).
4 M. B. Tsang, J. R. Stone, F. Camera, P. Danielewicz, S. Gandolfi, K. Hebeler, C. J. Horowitz, Jenny Lee, W. G. Lynch, Z. Kohley, R. Lemmon, P. Möller, T. Murakami, S. Riordan, X. Roca-Maza, F. Sammarruca, A. W. Steiner, I. Vidaña, and S. J. Yennello, Phys. Rev. C **86**, 015803 (2012).
5 J. M. Lattimer, and A. W. Steiner, Eur. Phys. J. A **50**, 40(2014).
6 Z. Zhang, and L. W. Chen, Phys. Lett. B **726**, 234 (2013).
7 P. Danielewicz, and J. Lee, Nucl. Phys. A **922**, 1 (2014).
8 X. Fan, J. Dong, and W. Zuo, Phys. Rev. C **89**, 017305 (2014).
9 X. H. Fan, J. M. Dong, and W. Zuo, Sci. China-Phys. Mech. Astron. **58**, 062002 (2015).
10 Z. Zhang, and L. W. Chen, Phys. Rev. C **92**, 031301 (2015).
11 N. Wang, M. Liu, L. Ou, and Y. Zhang, Phys. Lett. B **751**, 553 (2015).
12 Y. X. Zhang, C. S. Zhou, J. X. Chen, N. Wang, K. Zhao, and Z. X. Zhu, Sci. China-Phys. Mech. Astron. **58**, 112002 (2015).
13 B. Y. Sun, Sci. Sin. Phys. Mech. Astron. **46**, 012018 (2016).
14 J. M. Dong, and Y. Y. Zong, Sci. Sin. Phys. Mech. Astron. (in Chinese), **46**, 012019 (2016).
15 Z. Xiao, B. A. Li, L. W. Chen, G. C. Yong, and M. Zhang, Phys. Rev. Lett. **102**, 062502 (2009).
16 Z. Q. Feng, and G. M. Jin, Phys. Lett. B **683**, 140 (2010).
17 P. Russotto, P. Z. Wu, M. Zoric, M. Chartier, Y. Leifels, R. C. Lemmon, Q. Li, J. Łukasik, A. Pagano, P. Pawłowski, and W. Trautmann, Phys. Lett. B **697**, 471 (2011).
18 M. D. Cozma, Y. Leifels, W. Trautmann, Q. Li, and P. Russotto, Phys. Rev. C **88**, 044912 (2013).
19 W. J. Xie, J. Su, L. Zhu, and F. S. Zhang, Phys. Lett. B **718**, 1510 (2013).
20 Y. Wang, C. Guo, Q. Li, H. Zhang, Y. Leifels, and W. Trautmann, Phys. Rev. C **89**, 044603 (2014).
21 J. Xu, L. W. Chen, M. Y. B. Tsang, H. Wolter, Y. X. Zhang, J. Aichelin, M. Colonna, D. Cozma, P. Danielewicz, Z. Q. Feng, A. Le Fèvre, T. Gaitanos, C. Hartnack, K. Kim, Y. Kim, C. M. Ko, B. A. Li, Q. F. Li, Z. X. Li, P. Napolitani, A. Ono, M. Papa, T. Song, J. Su, J. L. Tian, N. Wang, Y. J. Wang, J. Weil, W. J. Xie, F. S. Zhang, and G. Q. Zhang, Phys. Rev. C **93**, 044609 (2016).
22 C. Guo, Y. Wang, Q. Li, and F. S. Zhang, Phys. Rev. C **90**, 034606 (2014).
23 Z. Chen, Y. Wang, C. Guo, and Q. Li, Sci. Sin.-Phys. Mech. Astron. **44**, 921 (2014).
24 G. F. Bertsch, and S. Das Gupta, Phys. Rept. **160**, 189 (1988).
25 J. Aichelin, C. Hartnack, A. Bohnet, Z. Li, G. Peilert, H. Stöcker, and W. Greiner, Phys. Lett. B **224**, 34 (1989).
26 S. A. Bass, et al. (PHENIX-Collaboration), Prog. Part. Nucl. Phys. **41**, 255 (1998).
27 M. Bleicher, et al. (PHENIX-Collaboration), J. Phys. G: Nucl. Part. Phys. **25**, 1859 (1999).
28 J. Aichelin, Phys. Rept. **202**, 233 (1991).
29 H. Sorge, H. Stöcker, and W. Greiner, Ann. Phys. 192, 266 (1989).
30 Q. Li, C. Shen, C. Guo, Y. Wang, Z. Li, J. Łukasik, and W. Trautmann, Phys. Rev. C **83**, 044617 (2011).

31 Y. Wang, C. Guo, Q. Li, and H. Zhang, Sci. China-Phys. Mech. Astron. **55**, 2407 (2012).
32 C. Guo, Y. Wang, Q. Li, W. Trautmann, L. Liu, and L. Wu, Sci. China-Phys. Mech. Astron. **55**, 252 (2012).
33 Y. Wang, C. Guo, Q. Li, H. Zhang, Z. Li, and W. Trautmann, Phys. Rev. C **89**, 034606 (2014).
34 M. Dutra, O. Lourenco, J. S. Sa Martins, A. Delfino, J. R. Stone, and P. D. Stevenson, Phys. Rev. C **85**, 035201 (2012).
35 W. Reisdorf, et al. (PHENIX-Collaboration), Nucl. Phys. A **876**, 1 (2012).
36 H. Kruse, B. V. Jacak, J. J. Molitoris, G. D. Westfall, and H. Stoecker, Phys. Rev. C **31**, 1770 (1985).
37 S. A. Bass, C. Hartnack, H. Stöcker, and W. Greiner, Phys. Rev. C **51** (1995) 3343.
38 W. Reisdorf, et al. (PHENIX-Collaboration), Nucl. Phys. A **781**, 459 (2007).